Rac GTPases regulate the morphology and deformability of the erythrocyte cytoskeleton

Theodosia A. Kalfa, Suvarnamala Pushkaran, Narla Mohandas, John H. Hartwig, Velia M. Fowler, James F. Johnson, Clinton H. Joiner, David A. Williams, and Yi Zheng

Actin oligomers are a significant structural component of the erythrocyte cytoskeleton. Rac1 and Rac2 GTPases regulate actin structures and have multiple overlapping as well as distinct roles in hematopoietic cells; therefore, we studied their role in red blood cells (RBCs). Conditional gene targeting with a *loxP*-flanked *Rac1* gene allowed Cre-recombinase–induced deletion of *Rac1* on a *Rac2* null genetic background. The *Rac1*$^{-/-}$;*Rac2*$^{-/-}$ mice developed microcytic anemia with a hemoglobin drop of about 20% and significant anisocytosis and poikilocytosis. Reticulocytes increased more than 2-fold. *Rac1*$^{-/-}$;*Rac2*$^{-/-}$ RBCs stained with rhodamine-phalloidin demonstrated F-actin meshwork gaps and aggregates under confocal microscopy. Transmission electron microscopy of the cytoskeleton demonstrated junctional aggregates and pronounced irregularity of the hexagonal spectrin scaffold. Ektacytometry confirmed that these cytoskeletal changes in *Rac1*$^{-/-}$;*Rac2*$^{-/-}$ erythrocytes were associated with significantly decreased cellular deformability. The composition of the cytoskeletal proteins was altered with an increased actin-to-spectrin ratio and increased phosphorylation (Ser724) of adducin, an F-actin capping protein. Actin and phosphorylated adducin of *Rac1*$^{-/-}$;*Rac2*$^{-/-}$ erythrocytes were more easily extractable by Triton X-100, indicating weaker association to the cytoskeleton. Thus, deficiency of Rac1 and Rac2 GTPases in mice alters actin assembly in RBCs and causes microcytic anemia with reticulocytosis, implicating Rac GTPases as dynamic regulators of the erythrocyte cytoskeleton organization. (Blood. 2006; 108:3637-3645)

Introduction

Rho GTPases, a subgroup of the Ras superfamily of small G proteins, function as molecular switches in a wide variety of signal transduction pathways in eukaryotic cells. Rho, Rac, and Cdc42, the most extensively studied members of this subgroup, control actin cytoskeleton; influence cell polarity and motility, microtubule dynamics, and vesicular transport pathways; and regulate cell survival, G_1 cell-cycle progression, and transcription.[1,2] Among the 3 members of mammalian Rac subfamily, Rac1 is ubiquitously expressed, Rac2 expression is restricted to cells of hematopoietic origin, and Rac3 is most highly expressed in the brain.[3,4] Rac1 affects cell spreading and adhesion of neutrophils,[5] whereas Rac2 regulates directed migration and superoxide production.[6,7] Rac1 and Rac2 GTPases play unique and overlapping roles in hematopoietic stem cells, where they differentially control engraftment, marrow retention, cell survival, and proliferation.[5,8] Many of the overlapping as well as distinct roles of Rac1 and Rac2 GTPases in hematopoietic cells are mediated through regulation of actin organization.

The erythrocyte membrane skeleton is organized as a hexagonal lattice of junctional complexes, each with the central component of a short actin filament, which are cross-linked by long, flexible spectrin molecules.[9] This thin network underlies the cytoplasmic surface of the plasma membrane and confers flexibility and strength to the membrane. Defects and deficiencies in components of this meshwork lead to fragile membranes and are associated with various hemolytic anemias.[10] The maintenance of normal membrane deformability and tensile strength is essential to permit the red blood cells (RBCs) to withstand shear forces in the circulation and to negotiate the microvasculature.

The junctional complex of the cytoskeleton is composed of a short actin filament (F-actin protofilament) and various actin-binding proteins. The length of the actin filaments is precisely maintained within a narrow Gaussian distribution,[11] indicating the existence of strict mechanisms that control the length of the F-actin filaments to an average of 12 to 18 actin monomers per oligomer, as well as the organization of about 6 spectrin molecules radiating from the central short protofilament to a regular hexagonal structure.[12] In vitro, actin polymerizes at the fast-growing (barbed) and slow-growing (pointed) filament ends. Among an array of actin interactive proteins, tropomodulin and adducin function as actin-capping proteins. They prevent actin monomer association or dissociation, thereby inhibiting the growth or shrinkage of protofilaments to maintain their length.[13]

The role of Rho GTPases in erythrocytes is largely unstudied. RhoA has been detected in both cytosol and membrane fractions of erythrocytes and has been found to bind specifically to the cytoplasmic surface of the RBC membrane with high affinity.[14] On the other hand, the Ras-related GTPase Rap1 has been recently implicated in RBC adhesion in sickle cell disease.[15] Of interest, Rap1 requires Rac1 to promote cell spreading in various cell types.[16]

From the Division of Experimental Hematology, Cincinnati Children's Research Foundation, Cincinnati Children's Hospital Medical Center and the University of Cincinnati College of Medicine, OH; New York Blood Center, New York, NY; Brigham and Women's Hospital, Harvard Medical School, Boston, MA; and The Scripps Research Institute, La Jolla, CA.

Submitted March 2, 2006; accepted July 12, 2006. Prepublished online as *Blood* First Edition Paper, August 1, 2006; DOI 10.1182/blood-2006-03-005942.

The publication costs of this article were defrayed in part by page charge payment. Therefore, and solely to indicate this fact, this article is hereby marked "advertisement" in accordance with 18 USC section 1734.

An Inside *Blood* analysis of this article appears at the front of this issue.

In the present study, we explored the role of Rac1 and Rac2 GTPases in RBC cytoskeleton regulation using a mouse gene-targeting approach. We found that the concurrent deficiency of Rac1 and Rac2 causes profound disruption of actin assembly and abnormal deformability of the erythrocyte cytoskeleton. We also found that increased phosphorylation of adducin on serine-724 (Ser724) is one of the mechanisms mediating these defects, indicating a dynamic regulation of the erythrocyte cytoskeleton organization.

Materials and methods

Reagents

Polyinosinic-polycytidylic acid (pI-pC) was purchased from Amersham-Pharmacia Biotech (Piscataway, NJ), Ca^{2+}-Mg^{2+}–free Dulbecco phosphate-buffer saline (PBS) from Gibco, Invitrogen (Carlsbad, CA); bovine serum albumin (BSA), Wright-Giemsa stain, glutaraldehyde, acrolein, phenylmethyl sulfonyl fluoride (PMSF), and poly-L-lysine (molecular weight range, 70-150 kDa) from Sigma-Aldrich (St Louis, MO); and ethylenediaminetetraacetic acid (EDTA)–coated microtiter tubes from Becton Dickinson (Rutherford, NJ). Monoclonal anti–β-actin antibody was obtained from Sigma-Aldrich; rabbit polyclonal GAPDH loading control antibody from Abcam (Cambridge, MA); rabbit polyclonal antiadducin antibody from BioLegend (San Diego, CA); mouse monoclonal anti–phospho-adducin (Ser724) from Upstate Biotechnology (Lake Placid, NY); mouse monoclonal antibodies for dematin and Rac1 from BD Transduction Laboratories (San Jose, CA); and rhodamine-phalloidin and Alexa-Fluor 488-conjugated anti–rabbit IgG from Molecular Probes (Eugene, OR). Rabbit polyclonal antibodies to spectrin, 4.1R, and tropomodulin were produced as previously described.[17-19] Rabbit polyclonal antibody to band 3 was kindly provided by Dr Philip Low (Purdue University, West Lafayette, IN). The monoclonal antibody for tropomyosin (CH1) developed by J. J.-C. Lin was obtained from the Developmental Studies Hybridoma Bank developed under the auspices of the National Institute of Child Health and Human Development (NICHD) and maintained by the University of Iowa, Department of Biological Sciences (Iowa City, IA). All the antibodies were used in 1:1000 dilution for immunoblotting, except the anti–β-actin antibody (1:2000) and the antitropomyosin antibody (1:500).

Mice and generation of Rac1-deficient erythrocytes in vivo

Mx1Cre$^{Tg/+}$;*Rac1*$^{flox/flox}$;*Rac2*$^{-/-}$ mice in a compound 129Sv and C57BL/6J background were generated as described previously.[5] Wild-type (WT), *Mx1Cre*$^{Tg/+}$;*Rac1*$^{flox/flox}$, and *Rac2*$^{-/-}$ mice of the same background were used as controls. These mice carry a bacteriophage *Cre* transgene driven by an IFN-γ–inducible *Mx1* promoter (designated as *Mx1Cre*$^{Tg/+}$),[20] which allows induction of Cre-recombinase expression in hematopoietic cells by intraperitoneal injections of pI-pC. All animal protocols were approved by the Institutional Animal Care and Use Committee of Cincinnati Children's Hospital Medical Center.

For deletion of *Rac1* sequence in vivo from hematopoietic cells including erythroid precursors, Cre-mediated recombination was carried out by pI-pC treatment of transgenic and WT mice as described previously,[5] with 5 intraperitoneal injections of 300 μg pI-pC administered every other day. *Rac2*$^{-/-}$ and WT mice were subjected to the same treatment to control for any effects of pI-pC independent of the Rac1 deletion.

Deletion of *Rac1* in mature RBCs after treatment with pI-pC was evaluated weekly by immunoblotting of washed packed RBCs (2 μL loaded/lane). RBCs were pelleted at 900 rpm (86*g*) for 5 minutes at room temperature, in an Eppendorf Centrifuge (Model 5417C, Eppendorf NorthAmerica, New York, NY), and after removal of the plasma and the top cell layer including the buffy coat, they were washed twice in PBS, pH 7.4.

Electrophoresis and Western blotting

Sodium dodecyl sulfate-polyacrylamide gel electrophoresis (SDS-PAGE) was performed according to the methods of Steck[21] or Laemmli[22] in 4-15% Tris-HCl polyacrylamide gradient gels (Bio-Rad Laboratories, Hercules, CA) with the following modification: urea-SDS sample buffer (1.3 M urea, 1.5% SDS, 40 mM Tris-HCl, 0.005% bromophenol blue), reduced (1% vol/vol 2-mercaptoethanol, 3 minutes at 100°C), was used to solubilize the samples; the presence of urea decreased smearing of the hemoglobin present in RBCs or pink ghosts samples. The gels were either stained with Coomassie blue or were transferred to PVDF membranes for immunoblotting. PVDF membranes were probed with various primary antibodies, followed by horseradish peroxidase (HRP)–conjugated secondary antibodies. Blots were developed with enhanced chemiluminescence reagents (ECL; Amersham Life Sciences, Arlington Heights, IL) and exposed in FujiFilm Intelligent Dark Box II, where the images were captured using Image Reader LAS-1000 software.

Measurement of the active (GTP-bound) Rac proteins

The level of active Rac1 protein in mature erythrocytes was measured by effector domain pull-down assay.[5,23] Briefly, the pull-down assay was performed by using the p21-binding domain (PBD) of the p21-activated kinase 1 (PAK1) fused with glutathione S-transferase (GST-PBD) bound to glutathione-agarose (Upstate Biotechnology) following the manufacturer's protocol.[24] GTP-bound Rac1 protein was analyzed by immunoblotting using anti-Rac1 antibody.

Hematologic analysis and histology

Peripheral-blood counts were determined using an automated hematology analyzer (Hemavet 850, Drew Scientific, Oxford, CT). A series of samples were also processed with an Advia Hematology Analyzer (Bayer HealthCare, Diagnostics Division, Tarrytown, NY), specifically calibrated for mouse blood, which provided histograms of RBC hemoglobin concentration and cellular volume. Whole blood was collected weekly in EDTA-coated microtiter tubes by tail or retro-orbital bleeding. Smears were stained with Wright-Giemsa stain. Reticulocytes were enumerated with flow cytometry after staining with thiazole orange (Retic-COUNT, Becton Dickinson, San Jose, CA) according to the manufacturer's protocol.

Spleens were placed in formalin 10% for fixation overnight and processed to paraffin. Sections (5 μm) were stained with hematoxylin and eosin for routine histologic examination and with Perls solution (1% potassium ferrocyanide in 1% hydrochloric acid) for detection of iron, counterstained with nuclear fast red (0.1% nuclear fast red, 5% aluminium sulfate in distilled water).

RBC ghost preparation and nonionic detergent elution of actin and adducin

Pink ghosts were prepared in the presence of $MgCl_2$ to protect actin filament capping, as previously described.[25] Washed RBCs were lysed with NaPi buffer (5 mM sodium phosphate, pH 7.4, containing 10 mM NaCl, 1 mM EGTA, 2 mM $MgCl_2$, and PMSF added fresh at a concentration of 20 μg/mL).[26] Erythrocyte ghost protein profile was studied by polyacrylamide gel electrophoresis. Three mice from each genetic group were used and 3 lanes of ghosts (20 μg total protein/lane) from each mouse were scanned. The results were averaged to minimize variations in gel loading, staining, and individual mouse phenotype. Coomassie blue–stained gels were scanned with a flat-bed scanner and densitometry was performed using NIH Image software (http://rsb.info.nih.gov/nih-image/).

Isolated pink ghosts (20 μg protein/sample) were incubated in NaPi buffer with 0.5% Triton X-100 for 60 minutes on ice. After centrifugation at 15 000*g* for 15 minutes, the actin and adducin, which were either associated with the cytoskeleton in the pellet (P) or extracted in the supernatant (S), were analyzed by SDS-PAGE and immunoblotting. The pellet was directly solubilized in urea-SDS sample buffer, whereas the protein in the supernatant was precipitated with acetone and then solubilized in urea-SDS sample buffer.

Measurements of cellular deformability by ektacytometry

Erythrocyte deformability was measured using an ektacytometer as described previously.[27,28] RBCs (within 24 hours from blood draw) were suspended in

dextran (40 000 M_r, 25% wt/vol) and deformed in a Couette viscometer, in which the outside cylinder is spun to obtain defined values of applied shear stress. The change in the laser diffraction pattern of the erythrocytes was recorded while they were subjected to increasing values of applied shear stress (0-250 dynes/cm^2). This photometric measurement produces a signal termed the deformability index (DI), a measure of the extent of cell deformation. The DImax, quantified as value of the DI attained at the maximum value of applied shear stress of 250 dynes/cm^2, is a measure of cellular deformability. Decreased values of DImax reflect decreased surface area-to-volume ratio and hence increased sphericity of RBCs.

Determination of cation content in erythrocytes

Net Na^+ and K^+ content was measured as previously described.[29] Briefly, cells were washed and resuspended at 2% hematocrit in HEPES-buffered saline. A triplicate sample was taken into isotonic $MgCl_2$ layered over dibutyl-phthalate. After centrifugation through the oil and washing, the cells were lysed in 4 mM $CsCl_2$. Hemolysate cation concentration was measured by flame emission (Perkin Elmer, Norwalk, CT, model 370 atomic absorption spectrophotometer). The hemoglobin concentration of each hemolysate, assayed optically at 540 nm on a Beckman Instruments DU spectrophotometer (Beckman Coulter, Fullerton, CA), was used to calculate cation content (millimoles) per kilogram of hemoglobin.

Immunofluorescence

Peripheral blood (4 μL) was diluted in 1 mL PBS containing 10 mM glucose and 1 mg/mL BSA, pH 7.4. BSA was added to the PBS solution because it preserves the biconcave shape of normal RBCs.[30] The cells were used for immunofluorescence staining within 18 hours of collection.

Immunofluorescence staining of erythrocytes was performed by 2 methods. The first included fixation of adhered blood cells on poly-L-lysine–coated coverslips with 0.5% glutaraldehyde in KCl solution (130 mM KCl, 20 mM K/Na phosphate buffer,10 mM glucose, 1 mg/mL BSA, pH 7.8) for 20 minutes, followed by staining with 2 U/slide rhodamine-phalloidin.[30] This produced a saturated staining of RBCs, which was informative of the erythrocyte morphology.

Specific immunofluorescence staining of RBCs for F-actin and band 3 was performed according to protocol previously described,[31] with modifications to allow staining of cells while attached on a coverslip, minimizing modification of the cell shape with repeated centrifugations. Peripheral blood cells were washed in PBS containing 10 mM glucose and 1 mg/mL BSA, pH 7.4, pelleted at 900 rpm (86*g*) for 5 minutes and fixed with 100 μL 0.5% acrolein in PBS for 5 minutes in solution. PBS with 10 mM glucose and 1 mg/mL BSA was added to adjust the amount of RBCs, in the final suspension to approximately 5×10^6 cells/mL. Glass coverslips were coated with 200 μL of 50μg/mL poly-L-lysine (molecular weight, 70-150 kDa) in PBS for 1 hour. Then 100 μL of the RBC suspension was applied per slide and allowed to adhere for 40 minutes at room temperature. Unbound cells were removed by rinsing thrice with PBS containing 0.1 M glycine (rinsing buffer). The erythrocytes were permeabilized in rinsing buffer containing 0.05% Triton X-100 for 10 seconds followed by rinsing 3 times in the same buffer without detergent. To ensure complete neutralization of unreacted aldehydes, cells were then incubated in rinsing buffer at room temperature for 30 minutes. Nonspecific binding was blocked by incubation for more than 60 minutes in blocking buffer (PBS containing 0.5 mM glycine, 0.2% fish skin gelatin, and 0.05% sodium azide). Fixed, permeabilized RBCs were stained for F-actin with rhodamine-phalloidin (0.05 U/slide) and for band 3 with anti–band 3 antibody (1:500 dilution). The slides stained for band 3 were rinsed 3 times with rinsing buffer and then incubated with secondary Alexa-Fluor 488-conjugated anti–rabbit IgG (4 μg/mL in blocking buffer). After final extensive rinsing the coverslips were mounted to glass slides using Fluoromount-G (Southern Biotechnology, Birmingham, AL).

The spatial distribution of the fluorescent probes was analyzed via 3-dimensional optical sectioning using a confocal laser-scanning microscope (LSM 510; Carl Zeiss, Thornwood, NY) with Zeiss LSM 510 software, version 3.2. Three-dimensional reconstruction (3D-rendering) and iterative deconvolution were applied to these images using Volocity software (Improvision, Lexington, MA). Volocity Classification was used to perform comparative measurements of the number of brightest fluorescent spots per cell in the samples stained with rhodamine-phalloidin. A classifier was created by choosing a minimal "intensity" (brightness) threshold and a minimal size of aggregates. The program uses these thresholds to identify the areas with these characteristics in every slice of the Z-stack processed. The classifier was validated by demonstrating the areas counted in the 3D-rendered image and confirming that the visible aggregates were selected.

Electron microscopy

Erythrocytes were attached to poly-L-lysine–coated glass coverslips by centrifugation at 200*g* for 5 minutes at room temperature. Glass-adherent erythrocytes were unroofed by attaching and removing a second poly-L-lysine–coated coverslip to their surface in PHEM (60 mM PIPES, 25 mM HEPES, 10 mM EGTA, and 2 mM $MgCl_2$, pH 6.9) containing 1 μM phallacidin at 37°C. Unroofed erythrocytes were extensively washed in PHEM, fixed with 1% glutaraldehyde in PBS for 10 minutes, washed into distilled water, rapidly frozen, freeze-dried, and rotary shadowed with 1.2 nm tungsten-tantalum at 45° followed by 3 nm carbon at 90° without rotation. Replicas were photographed with an electron microscope (model 1200-EX; JEOL USA, Peabody, MA) at a 100-kV accelerating voltage.

Statistics

All values are presented as the mean ± SEM. Statistical significance was evaluated using *t* test to compare the posttreatment hematologic parameters of a group versus the pretreatment ones and using ANOVA test to compare the hematologic parameters of the 4 groups studied (WT, $Rac1^{-/-}$, $Rac2^{-/-}$, $Rac1^{-/-}$;$Rac2^{-/-}$) before and after treatment. Results were considered significantly different at $P < .05$.

Results

Homozygous Rac1-deficient mice die before embryonic day 9 (E9) in utero.[32] Therefore, to study Rac1 deficiency in mature erythrocytes, we used mice with a conditional *Rac1* (flox) allele[33] and a transgene for bacteriophage Cre recombinase expressed via an IFN-γ–inducible *Mx1* promoter (designated as $Cre^{Tg/+}$).[20] These mice ($Cre^{Tg/+}$;$Rac1^{flox/flox}$) were crossed into $Rac2^{-/-}$ mice to yield the experimental genotype $Cre^{Tg/+}$;$Rac1^{flox/flox}$;$Rac2^{-/-}$. Cre-mediated recombination was carried out by 5 intraperitoneal injections of pI-pC at a dose of 300 μg every other day, as described previously.[5] $Rac1^{flox/flox}$, $Rac2^{-/-}$, and WT mice were also subjected to the same treatment to achieve *Rac1* deletion or to control for any effects of pI-pC independent of the *Rac1* deletion. Absence of *Rac2* sequences in the $Cre^{Tg/+}$;$Rac1^{flox/flox}$;$Rac2^{-/-}$ and the $Rac2^{-/-}$ mice was confirmed by polymerase chain reaction (PCR) genotyping as previously described[6,34] (data not shown). Expression of Rac1 protein after treatment with pI-pC was analyzed by immunoblotting in washed RBCs. The time of maximum Rac1 deficiency in erythrocytes was determined to be 2 to 5 weeks after pI-pC treatment. During this period, Rac1 protein level in the erythrocytes of the $Cre^{Tg/+}$;$Rac1^{-/-}$;$Rac2^{-/-}$ mice was decreased to 20% to 50% of the corresponding WT level, as determined by densitometry (Figure 1A). We confirmed with PBD pull-down assay that active (GTP-bound) Rac1 was similarly or even more significantly decreased (Figure 1B).

Hematologic analysis

The pI-pC–treated $Rac1^{-/-}$;$Rac2^{-/-}$ mice developed a mild microcytic anemia with a drop in hemoglobin concentration of 15% to 20% (Table 1). Microcytosis was noted at baseline in $Rac2^{-/-}$ and $Rac1^{flox/flox}$;$Rac2^{-/-}$ mice. The mean corpuscular volume (MCV) of

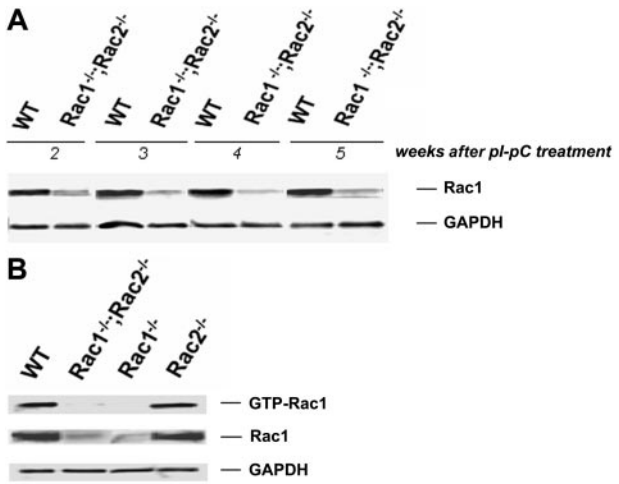

Figure 1. Cre-mediated deletion of *Rac1* sequence after pI-pC treatment. (A) Rac1 protein as detected by immunoblotting in WT and *Rac1*$^{-/-}$*;Rac2*$^{-/-}$ washed RBC samples obtained weekly over the period of 2 to 5 weeks after induction. GAPDH used as loading control. Data representative of 12 samples tested per week. (B) Active, GTP-bound Rac1 determined by PBD pull-down assay 3 weeks after pI-pC treatment. Genotypes shown above. GAPDH used as loading control. Data representative of 3 experiments with similar results.

Rac1$^{-/-}$*;Rac2*$^{-/-}$ erythrocytes decreased after pI-pC treatment by about 20% in comparison with WT and by about 10% in comparison with baseline, whereas the RBC distribution width (RDW) increased significantly, reflecting the poikilocytosis and RBC fragmentation that was also evident on blood smears (Figure 2A). The percentage of reticulocytes in *Rac1*$^{-/-}$*;Rac2*$^{-/-}$ mice increased more than 2-fold and the spleen weight doubled (Table 1). Iron staining showed increased iron deposition in the *Rac1*$^{-/-}$*; Rac2*$^{-/-}$ spleen (Figure 2D), consistent with increased hemolysis. White blood cell counts were significantly elevated in *Rac1*$^{-/-}$*; Rac2*$^{-/-}$ mice, as previously described in *Rac2*$^{-/-}$ and transgenic *Rac1*$^{-/-}$*;Rac2*$^{-/-}$ mice.[5,6,35] Significant anisocytosis, poikilocytosis, and polychromasia, as well as hypochromic cells, target cells, and fragmented erythrocytes were observed on stained *Rac1*$^{-/-}$*; Rac2*$^{-/-}$ blood smears (Figure 2A). Mice lacking either Rac1 or Rac2 GTPase alone demonstrated a minimal anemia with no significant reticulocytosis and only mild changes of erythrocyte morphology. A mild microcytosis was noted in the *Rac2*$^{-/-}$ mice suggesting some unique although subtle role of Rac2 in erythrocytes (Table 1; Figure 2A).

Blood samples from WT and *Rac1*$^{-/-}$*;Rac2*$^{-/-}$ mice were also analyzed with an Advia Hematology Analyzer, which uses optical light scattering to derive RBC volume and cell-hemoglobin concentration on a cell-by-cell basis. Corpuscular hemoglobin concentration mean (CHCM) and hemoglobin concentration distribution width (HDW) were calculated as the mean and the width of the hemoglobin concentration histogram, respectively, along with the RBC count. Representative histograms of the RBC volume and hemoglobin concentration are shown in Figure 2B. A population of small (left-shifted volume distribution) RBCs was present in *Rac1*$^{-/-}$*;Rac2*$^{-/-}$ blood compared with WT, indicating probable loss of membrane. CHCM was similar in WT and *Rac1*$^{-/-}$*; Rac2*$^{-/-}$ mice (281 ± 5 g/L [28.1 ± 0.5 g/dL] versus 276 ± 3 g/L [27.6 ± 0.3 g/dL]), but HDW was significantly broadened (18.4 ± 0.3 g/L [1.84 ± 0.03 g/dL] versus 26.3 ± 2.5 g/L [2.63 ± 0.25 g/dL]; $P < .05$). These data suggest the presence of microspherocytes with increased corpuscular hemoglobin concentration as well as the presence of hypochromic cells. On the other hand, the intracellular sodium and potassium content (normalized to hemoglobin), as measured by flame-emission spectroscopy, was normal (data not shown), suggesting no major abnormalities in cation transport or volume regulation.

Immunofluorescent images of erythrocytes fixed with glutaraldehyde and stained with rhodamine-phalloidin were obtained by confocal microscopy and subjected to 3-dimensional reconstruction (Figure 2C). These images confirmed that *Rac1*$^{-/-}$*;Rac2*$^{-/-}$ erythrocytes display a significant anisocytosis and poikilocytosis as well as a high frequency of abnormal microspherocytes with punctuate lesions or irregularly shaped fragmented cells.

Table 1. Hematologic parameters in control and experimental mice before (baseline) and 3 weeks after treatment with pI-pC

Genotype	No.	Hgb level, g/L	MCV, fL	RDW, %	Reticulocytes, %	Spleen weight, %
Before pI-pC						
WT	12	165 ± 4	55.3 ± 0.4	19.7 ± 0.2	2.6 ± 0.2	—
Rac1$^{flox/flox}$	6	164 ± 3	51.8 ± 0.7	19.6 ± 0.4	2.9 ± 0.3	—
Rac2$^{-/-}$	6	153 ± 4	50.4 ± 0.5[a]	21.3 ± 0.4[b]	3.4 ± 0.2	—
Rac1$^{flox/flox}$*; Rac2*$^{-/-}$	12	154 ± 3	48.8 ± 0.7[c]	20.4 ± 0.3	3.1 ± 0.2	—
After pI-pC						
WT	12	160 ± 3	56.9 ± 1.0	18.6 ± 0.6	3.8 ± 0.3[d]	0.36 ± 0.03
Rac1$^{-/-}$	6	155 ± 2[e]	54.2 ± 0.5[e]	21.2 ± 0.7	3.9 ± 0.2[e]	0.43 ± 0.07
Rac2$^{-/-}$	6	142 ± 5[f]	49.6 ± 0.9[g]	21.5 ± 0.7	4.8 ± 0.5[h]	0.37 ± 0.03
Rac1$^{-/-}$*; Rac2*$^{-/-}$	12	128 ± 3[ij]	43.3 ± 0.6[ij]	28.1 ± 1.4[ij]	7.2 ± 0.4[ij]	0.72 ± 0.15[k]

All values are mean ± SEM. Population is 12 for the groups of WT and *Mx1Cre*$^{Tg/+}$*; Rac1*$^{flox/flox}$*; Rac2*$^{-/-}$ mice and 6 for the groups of *Mx1Cre*$^{Tg/+}$*; Rac1*$^{flox/flox}$ and *Rac2*$^{-/-}$ mice. Corresponding Rac1 protein levels by densitometry after treatment with pI-pC, at the time these blood counts were obtained, were 99.9 ± 1.8% for the WT mice and 42.3 ± 3.5% (range, 25.6%-56.8%) for the *Rac1*$^{-/-}$*; Rac2*$^{-/-}$ mice. Spleen weight was evaluated for 6 mice per group and is expressed as percent of the body weight.

To convert hemoglobin level from grams per liter to grams per deciliter, divide grams per liter by 10.

— indicates not determined. Spleen size within normal limits was observed for all genotypes before pI-pC treatment.

[a] $P < .05$ versus WT at baseline.

[b] $P < .05$ versus WT and *Rac1*$^{-/-}$ at baseline.

[c] $P < .05$ versus WT and *Rac1*$^{-/-}$ at baseline.

[d] $P < .05$ versus WT at baseline.

[e] $P < .05$ versus *Rac1*$^{flox/flox}$ at baseline.

[f] $P < .05$ versus WT after pI-pC treatment.

[g] $P < .05$ versus WT and *Rac1*$^{-/-}$ after pI-pC treatment.

[h] $P < .05$ versus *Rac2*$^{-/-}$ at baseline.

[i] $P < .05$ versus WT, *Rac1*$^{-/-}$, and *Rac2*$^{-/-}$ after pI-pC treatment.

[j] $P < .001$ versus *Rac1*$^{flox/flox}$*; Rac2*$^{-/-}$ at baseline.

[k] $P < .05$ versus WT after pI-pC treatment.

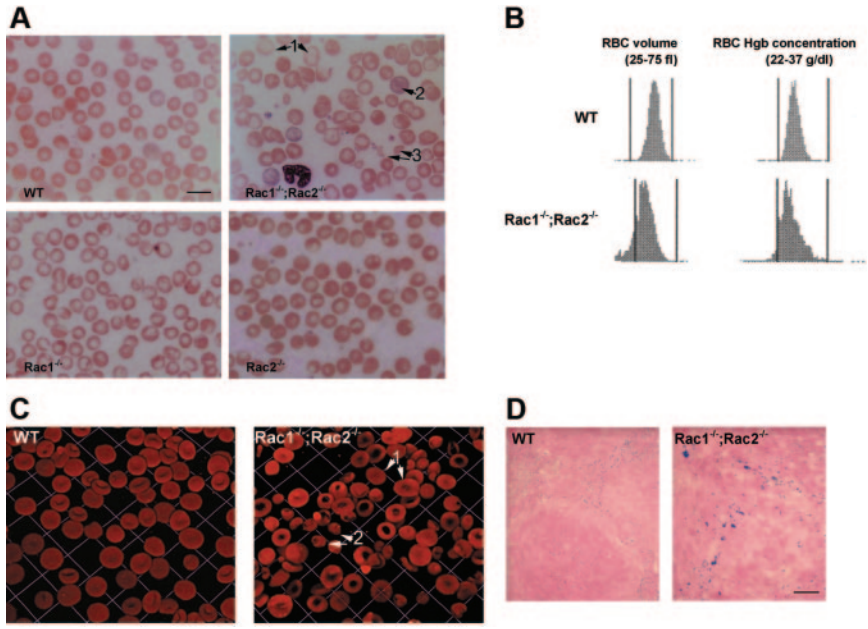

Figure 2. Abnormal morphology of *Rac1*$^{-/-}$;*Rac2*$^{-/-}$ erythrocytes. (A) Wright-Giemsa staining of blood smears of WT, *Rac1*$^{-/-}$, *Rac2*$^{-/-}$, and *Rac1*$^{-/-}$;*Rac2*$^{-/-}$ mice. *Rac1*$^{-/-}$ and *Rac2*$^{-/-}$ blood smears show mild poikilocytosis and anisocytosis. The *Rac1*$^{-/-}$;*Rac2*$^{-/-}$ blood smear demonstrates severe poikilocytosis; arrows indicate the presence of hypochromia (1), polychromasia (2), and fragmented cells (3). Scale bar represents 10 μm. (B) RBC volume and hemoglobin concentration histograms obtained by automated complete blood count analysis of WT and *Rac1*$^{-/-}$;*Rac2*$^{-/-}$ whole blood with an Advia Hematology Analyzer (images representative of 6 samples tested for each genotype). (C) Three-dimensional reconstruction of glutaraldehyde-fixed erythrocyte images. Images were obtained with a × 100 oil-immersed objective lens, numerical aperture 1.45. Arrows show *Rac1*$^{-/-}$;*Rac2*$^{-/-}$ erythrocytes with thinned appearance especially at the central area (1), and a high frequency of bizarre microspherocytes with punctuate lesions (2). One unit represents 9.2 μm. (D) Increased iron deposits in the spleen of *Rac1*$^{-/-}$;*Rac2*$^{-/-}$ mice compared with WT. Scale bar represents 100 μm.

Erythrocyte deformability

Ektacytometry of *Rac1*$^{-/-}$;*Rac2*$^{-/-}$ RBCs also showed significant abnormalities. The maximum value of the deformability index (DImax) was decreased to an average of 81% of the control WT cells indicating reduced cellular deformability, whereas erythrocytes deficient in only Rac1 or only Rac2 exhibited normal cellular deformability (Figure 3). We concluded that a normal activity of either Rac1 or Rac2 GTPase was sufficient to maintain normal membrane stability, but deficiency of both proteins results in decreased membrane mechanical stability leading to cell-surface area loss and decreased cellular deformability. Therefore, we focused additional studies on the *Rac1*$^{-/-}$;*Rac2*$^{-/-}$ RBCs.

Erythrocyte cytoskeleton analysis

Because Rac GTPases have been shown to regulate actin structures in other hematopoietic cells, we explored the distribution of the actin oligomers in the erythrocyte cytoskeleton, using rhodamine-phalloidin staining of acrolein-fixed erythrocytes (Figure 4A). The actin meshwork in WT cells appeared regular, symmetrical, and smooth. In contrast, obvious meshwork gaps and aggregates of F-actin were present in the *Rac1*$^{-/-}$;*Rac2*$^{-/-}$ erythrocyte cytoskeleton. We counted the number of the brightest fluorescent spots per cell in the samples stained with rhodamine-phalloidin and identified an average of 4 spots/cell in the WT cells in contrast to an average of 23.8 spots/cell in the *Rac1*$^{-/-}$;*Rac2*$^{-/-}$ cells. In agreement with the irregularity of the horizontal cytoskeleton meshwork, the distribution of the transmembrane protein band 3 in *Rac1*$^{-/-}$;*Rac2*$^{-/-}$ erythrocytes appeared irregular with obvious clumping (Figure 4B). Transmission electron microscopy of the erythrocyte cytoskeleton demonstrated the presence of structures resembling junctional aggregates, pronounced irregularity of the hexagonal spectrin scaffold, and a paucity of membrane "endo-vesiculations" (Figure 5).

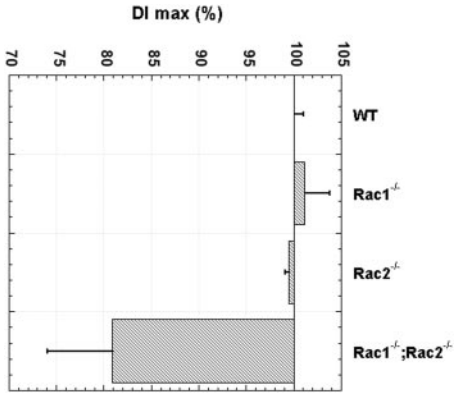

Figure 3. Reduced deformability index of *Rac1*$^{-/-}$;*Rac2*$^{-/-}$ erythrocytes. Ektacytometry of *Rac1*$^{-/-}$;*Rac2*$^{-/-}$ RBCs was used to determine the maximum value of deformability index (DImax). Results are expressed as mean ± SD of 12 *Rac1*$^{-/-}$;*Rac2*$^{-/-}$ blood samples and 6 WT, *Rac1*$^{-/-}$, *Rac2*$^{-/-}$ blood samples obtained 2 weeks after completion of treatment with pI-pC. $P < .001$ by *t* test for the difference between *Rac1*$^{-/-}$;*Rac2*$^{-/-}$ and WT. *Rac1*$^{-/-}$ and *Rac2*$^{-/-}$ blood samples had no statistically significant difference from WT.

Cytoskeletal protein analysis and phosphorylation profile

Rho GTPases, including Rac, are regulators of a number of signaling pathways in nonhematopoietic and nonerythroid hematopoietic cells. To assess the potential role of Rac signaling pathways required for maintenance of the erythrocyte cytoskeleton, we analyzed the cytoskeletal protein composition and phosphorylation changes of adducin, which is the actin-capping protein of the fast-growing (barbed) end in RBCs. The erythrocyte ghost protein profile was evaluated in SDS-polyacrylamide gels (Figure 6A). The actin-to-spectrin ratio was increased an average of 2.6-fold in *Rac1*$^{-/-}$;*Rac2*$^{-/-}$ ghosts versus WT ghosts. Further analysis of actin-interacting cytoskeletal proteins was performed by immunoblotting (Figure 6B). *Rac1*$^{-/-}$;*Rac2*$^{-/-}$ erythrocytes demonstrated decreased membrane content of adducin and dematin in comparison to WT cells, whereas the content of protein 4.1R, tropomodulin, and tropomyosin was unchanged. However, the stoichiometric ratio of actin to all actin-interacting proteins examined appeared increased in *Rac1*$^{-/-}$; *Rac2*$^{-/-}$ RBCs. Serine phosphorylation of adducin was additionally studied in WT and *Rac1*$^{-/-}$;*Rac2*$^{-/-}$ erythrocytes. An antibody recognizing phosphorylated Ser724 of α-adducin and similar sequence within β- and γ-adducin isoforms revealed increased phosphorylation of adducin on Ser724 in

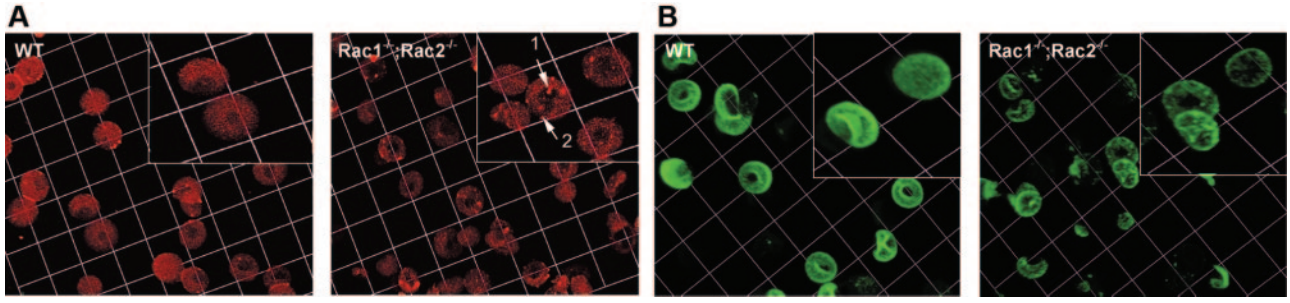

Figure 4. Cytoskeleton structure of *Rac1*$^{-/-}$*;Rac2*$^{-/-}$ erythrocytes. (A) Erythrocytes fixed with acrolein and stained with rhodamine-phalloidin for F-actin. Arrowheads in magnified inset show meshwork gaps and aggregates of F-actin in *Rac1*$^{-/-}$*;Rac2*$^{-/-}$ erythrocytes. (B) RBCs stained with anti–band 3 antibody to visualize band 3 distribution. Images were obtained with a × 63 oil-immersed objective lens, software zoom × 2, numerical aperture 1.4; 1 unit represents 7.3 μm.

Rac1$^{-/-}$*;Rac2*$^{-/-}$ erythrocytes (Figure 6B). Actin and phosphorylated adducin (Ser724) were more soluble in *Rac1*$^{-/-}$*;Rac2*$^{-/-}$ RBCs as determined by extraction with a nonionic detergent as Triton X-100 (Figure 6C). These data suggest that deficiency of Rac1 and Rac2 caused defects in the organization of actin in the erythrocyte cytoskeleton. In these cells, although more actin was present, the association of actin with spectrin was weaker, and this defective interaction was associated with increased phosphorylation of adducin on Ser724.

Discussion

Rho GTPases regulate the actin cytoskeleton in a wide variety of cell types. The best-studied Rho GTPases are RhoA, Rac1, and Cdc42. RhoA activity has been shown to induce the assembly of contractile actin and myosin filaments (stress fibers), whereas Rac1 and Cdc42 promote the formation of surface protrusions (lamellipodia and membrane ruffles) and fingerlike membrane extensions (filopodia), respectively.[2,37] The 3 highly related Rac GTPases, Rac1, Rac2, and Rac3, are distributed in different patterns.[37] Rac1 is ubiquitously expressed, Rac3 is most highly expressed in the brain, and Rac2 is exclusively expressed in hematopoietic tissues.[2] In hematopoietic cells it has been shown that Rac1 and Rac2 GTPases are responsible for distinct as well as some overlapping functions.[5,8,38,39] It is clear from the studies reported here that in RBCs, Rac1 and Rac2 share overlapping functions to maintain normal membrane stability and hence normal cellular deformability. A mild microcytosis noted in the Rac2-deficient erythrocytes may indicate a unique although subtle role of Rac2 as well. Although gene deletion of both *Rac1* and *Rac2* resulted in a clear cytoskeleton phenotype, the role of Rac3 in the RBC actin meshwork regulation remains to be determined using *Rac3* gene-targeted mice in the future.[40,41]

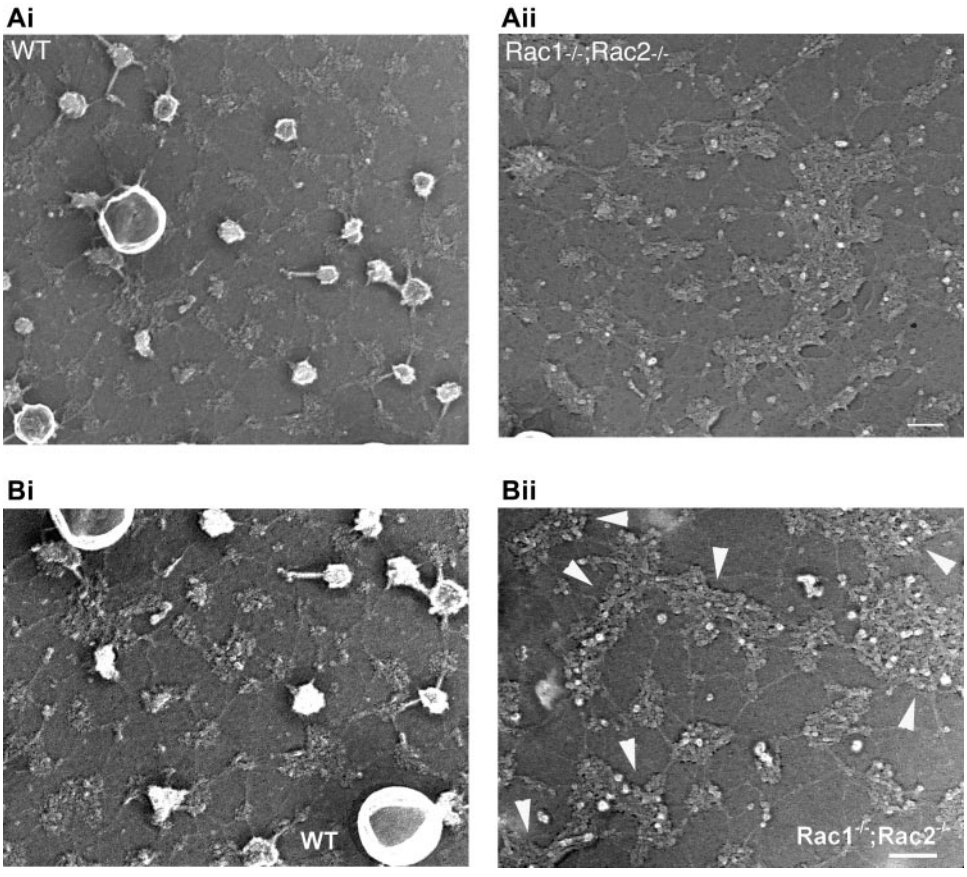

Figure 5. Organization of the membrane skeletons of WT and *Rac1*$^{-/-}$*;Rac2*$^{-/-}$ erythrocytes. Micrographs of representative metal cast of a WT and a *Rac1*$^{-/-}$*; Rac2*$^{-/-}$ unroofed erythrocyte. (A) The membrane skeleton of the WT erythrocyte is composed of a uniform lattice of interconnected strands, as previously reported.[36] *Rac1*$^{-/-}$*;Rac2*$^{-/-}$ membrane skeletons revealed irregularity of the hexagonal spectrin scaffold and a paucity of membrane "endovesiculations." Scale bar represents 100 nm. (B) In higher magnification, the arrowheads point to large clusters in the *Rac1*$^{-/-}$*; Rac2*$^{-/-}$ cytoskeleton that appear to have the same "globular" consistency with the junctions in the WT cytoskeleton. Scale bar represents 100 nm.

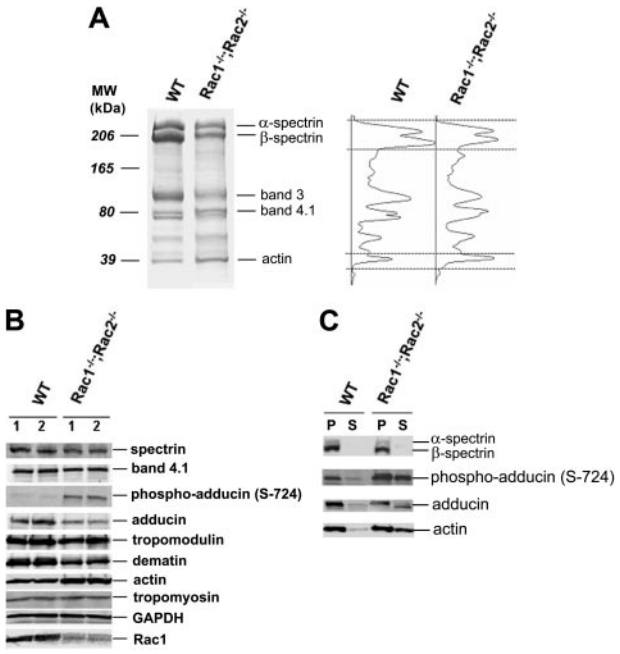

Figure 6. Erythrocyte protein and phosphorylation profile in *Rac1*$^{-/-}$;*Rac2*$^{-/-}$ RBCs evaluated in SDS-polyacrylamide gels. (A) RBC ghost electrophoretic pattern in *Rac1*$^{-/-}$;*Rac2*$^{-/-}$ versus WT erythrocytes. Molecular weight markers and major RBC cytoskeleton proteins are indicated. Densitometry scans of the 2 lanes, respectively, are shown on the right with spectrin and actin bands noted between the dotted lines. The actin-to-spectrin ratio was reproducibly 2 to 3 times higher in the *Rac1*$^{-/-}$;*Rac2*$^{-/-}$ ghosts versus the WT ghosts. (B) Profile of the major actin-interacting proteins and serine phosphorylation of adducin in WT and *Rac1*$^{-/-}$;*Rac2*$^{-/-}$ erythrocytes (2 μL packed RBCs loaded/lane). Two different samples from each genotype are shown. (C) Triton-soluble (S) and pellet (P) fractions of erythrocyte ghosts evaluated by immunoblotting for the presence of spectrin, adducin, actin, and phospho-adducin (Ser724). All images are representative of at least 6 different blood samples from each genotype.

A technical problem with the inducible gene-targeting approach to achieve Rac1 protein depletion is the persistence of "preinduction" RBCs in the circulation. A 2-week interval was necessary for the circulating RBC renewal so we could observe a significant reduction in erythrocyte Rac1 level and the associated changes in erythrocyte phenotype. Furthermore, the phenotype was transient. Five to 6 weeks after pI-pC treatment, we observed an increase of Rac1 protein in the *Rac1*$^{flox/flox}$;*Rac2*$^{-/-}$ blood cells. This phenomenon is in agreement with previous observations that the *Rac1*^{flox} allele reappears in the peripheral blood of pI-pC–treated *Mx1Cre*$^{Tg/+}$;*Rac1*$^{flox/flox}$;*Rac2*$^{-/-}$ mice 3 to 7 weeks after treatment,[8] possibly due to a strong selective pressure in vivo for a residual population of non-*Rac1*–deleted hematopoietic stem cells in the setting of concurrent absence of Rac2 activity. Therefore, we focused our studies in the period of 2 to 5 weeks after pI-pC treatment with a close monitoring of Rac1 protein level in the RBCs.

Rac1$^{-/-}$;*Rac2*$^{-/-}$ mice developed anemia with concurrent evidence of hemolysis: presence of fragmented cells in the smear, reticulocytosis, and increased iron depositions in the spleen. RBC volume and cell-hemoglobin concentration as depicted by the smear and erythrocyte indices indicated the presence of microspherocytes with loss of membrane and increased corpuscular hemoglobin concentration, as well as the presence of young hypochromic cells. Ektacytometry was also abnormal for the *Rac1*$^{-/-}$;*Rac2*$^{-/-}$ erythrocytes. WT erythrocytes and cells deficient in only Rac1 or Rac2 had a normal DImax, which is a direct measure of the RBC membrane surface area-to-volume ratio,[27] whereas *Rac1*$^{-/-}$;*Rac2*$^{-/-}$ RBCs had a significantly decreased DImax as a result of cell-surface area loss. Confocal microscopy images provided a visual demonstration of a high frequency of bizarre microspherocytes with probable shedding of microvesicles. These results implicate Rac1 and Rac2 GTPases in maintaining normal membrane deformability and mechanical stability, which is critical for the ability of RBCs to undergo extensive deformations in the microvasculature.

The RBC cytoskeleton underlies and supports the membrane as a hexagonal scaffold of actin oligomers (located on the junctions) cross-linked by long, flexible spectrin molecules. Meshwork gaps and aggregates of F-actin in the *Rac1*$^{-/-}$;*Rac2*$^{-/-}$ erythrocyte cytoskeleton were demonstrated by confocal microscopy with immunofluorescent labeling. Structures resembling junctional aggregates were notable in transmission electron microscopy images of the cytoskeleton along with pronounced irregularity of the hexagonal spectrin scaffold and a paucity of membrane "endo-vesiculations." In agreement with the irregularity of the horizontal cytoskeleton meshwork, the transmembrane protein band 3 distribution in the *Rac1*$^{-/-}$;*Rac2*$^{-/-}$ erythrocytes was also irregular with areas of apparent clumping, reminiscent of the band 3 clustering that has been shown in nonimmune hemolytic anemias to lead to autologous antibody formation and binding, phagocytosis, and shorter erythrocyte life span.[42,43]

These morphologic observations indicate that Rac GTPases regulate the actin organization into oligomers in the erythrocyte cytoskeleton. In agreement with the cytoskeletal structure perturbations, the stoichiometric ratio of actin to other cytoskeletal proteins, especially spectrin, adducin, and dematin in *Rac1*$^{-/-}$;*Rac2*$^{-/-}$ erythrocytes was increased. Additionally, the actin in *Rac1*$^{-/-}$;*Rac2*$^{-/-}$ ghosts was more soluble in nonionic detergent, indicating that in the absence of normal activity of Rac1 and Rac2 the association of actin-spectrin scaffold is defective.

The actin protofilaments in the erythrocyte cytoskeleton are stabilized at the rapidly exchanging (barbed) ends by adducin[44,45] and at the slow-exchanging (pointed) ends by tropomodulin.[26,46] Adducin was originally identified as a calmodulin-binding protein in erythrocytes,[47] but it is expressed in many cell types[48,49] where it forms along with spectrin and F-actin a meshwork beneath the plasma membrane and may participate in the formation of membrane ruffling.[50] Phosphorylation changes of adducin have been shown to regulate actin-spectrin association in several cell types. Phosphorylation of α-adducin on threonine (Thr445 and Thr480) in canine kidney epithelial cells by Rho kinase, a downstream target of Rho GTPase, enhances the F-actin–binding activity of adducin and promotes recruitment of spectrin to F-actin.[50,51] In contrast, phosphorylation of adducin on Ser726 in human platelets (corresponding to Ser724 for mouse α-adducin) causes dissociation of spectrin from actin.[52] We demonstrated increased phosphorylation of adducin on Ser724 in *Rac1*$^{-/-}$;*Rac2*$^{-/-}$ erythrocytes. Phosphorylated adducin was also more readily extractable from the ghost cytoskeleton by Triton X-100, in the Rac-deficient cells. Ser724 is a major phosphorylation site in the COOH-terminal domain of adducin, called myristoylated alanine-rich C kinase substrate (MARCKS) domain, and a substrate of both protein kinase C (PKC) and protein kinase A (PKA).[53,54] The MARCKS domain, when not phosphorylated, caps the fast-growing ends of actin filaments and preferentially recruits spectrin.[44,54,55] However, once phosphorylated on Ser724 it releases from F-actin and spectrin as has been demonstrated in the case of platelet activation,[52] and as we report here in *Rac1*$^{-/-}$;*Rac2*$^{-/-}$ erythrocytes. Additionally, it has been reported that adducin phosphorylated in the MARCKS domain is proteolyzed by calpain in platelets,[56] whereas in renal epithelial cells phosphorylated α-adducin is cleaved by caspase to

generate a 74-kDa fragment that renders its dissociation from the cytoskeleton irreversible.[57] Such a proteolytic mechanism may also be at work in our observation that total amount of adducin decreases in *Rac1*$^{-/-}$*;Rac2*$^{-/-}$ erythrocytes.

In conclusion, Rac1 and Rac2 GTPases modulate the erythrocyte cytoskeleton dynamics, likely through pathways that target F-actin protofilament capping. Various genetic mutations of structural cytoskeletal proteins have been associated with hereditary spherocytosis, eliptocytosis, and pyropoikilocytosis syndromes. However, in a number of kindreds the defect has not been elucidated. Some of these idiopathic membrane defects might be explained by alterations of signaling pathways that modulate phosphorylation of cytoskeletal components, and to this end Rac GTPases and their downstream effectors are possible candidates. Additionally, the role and significance of Rac signaling in modifying inherited or acquired hemolytic anemias with a known etiology requires further investigation. Our data imply a dynamic regulation of the RBC cytoskeleton by intracellular signaling molecules. Elucidation of these pathways may offer new insights in erythrocyte physiology and pathology and provide possible targets for treatment of hemolytic anemias.

Acknowledgments

The authors thank Dr Philip Low, Dr Samuel Lux, and Dr Jose Cancelas for valuable discussion and suggestions.

This work was supported by the National Institutes of Health R01 grants GM60523, DK62757, and DK26263. T.A.K. was supported by training grants from the National Heart, Lung and Blood Institute (U54 HL70871) for Sickle Cell Scholars Program and National Institute of Child Health and Human Development (K12 HD28827).

Authorship

T.A.K. designed and performed research, analyzed data, and wrote the paper; S.P. and J.F.J. performed research and analyzed data; N.M. directed and analyzed ektacytometry studies, and contributed valuable reagents and advice for data analysis and the writing of the manuscript; J.H.H. performed electron microscopy experiments and offered valuable insights; V.M.F. contributed valuable reagents and insights; C.H.J. directed and analyzed determination of RBC cation content experiments and offered valuable advice for data analysis and the writing of the manuscript; and D.A.W. and Y.Z. were instrumental in experimental design, data analysis, and the writing of the manuscript.

The authors declare no competing financial interests.

Correspondence: Theodosia A. Kalfa, Division of Experimental Hematology, Cincinnati Children's Hospital Medical Center, 3333 Burnet Ave, MLC 7015, Cincinnati, OH 45229; e-mail: theodosia.kalfa@cchmc.org.

References

1. Etienne-Manneville S, Hall A. Rho GTPases in cell biology. Nature. 2002;420:629-635.
2. Burridge K, Wennerberg K. Rho and Rac take center stage. Cell. 2004;116:167-179.
3. Moll J, Sansig G, Fattori E, van der Putten H. The murine rac1 gene: cDNA cloning, tissue distribution and regulated expression of rac1 mRNA by disassembly of actin microfilaments. Oncogene. 1991;6:863-866.
4. Shirsat NV, Pignolo RJ, Kreider BL, Rovera G. A member of the ras gene superfamily is expressed specifically in T, B and myeloid hemopoietic cells. Oncogene. 1990;5:769-772.
5. Gu Y, Filippi MD, Cancelas JA, et al. Hematopoietic cell regulation by Rac1 and Rac2 guanosine triphosphatases. Science. 2003;302:445-449.
6. Roberts AW, Kim C, Zhen L, et al. Deficiency of the hematopoietic cell-specific Rho family GTPase Rac2 is characterized by abnormalities in neutrophil function and host defense. Immunity. 1999;10:183-196.
7. Williams DA, Tao W, Yang F, et al. Dominant negative mutation of the hematopoietic-specific Rho GTPase, Rac2, is associated with a human phagocyte immunodeficiency. Blood. 2000;96:1646-1654.
8. Cancelas JA, Lee AW, Prabhakar R, Stringer KF, Zheng Y, Williams DA. Rac GTPases differentially integrate signals regulating hematopoietic stem cell localization. Nat Med. 2005;11:886-891.
9. Byers TJ, Branton D. Visualization of the protein associations in the erythrocyte membrane skeleton. Proc Natl Acad Sci U S A. 1985;82:6153-6157.
10. Mohandas N, Evans E. Mechanical properties of the red cell membrane in relation to molecular structure and genetic defects. Annu Rev Biophys Biomol Struct. 1994;23:787-818.
11. Lux SE, Palek J. Disorders of the red cell membrane. In: Handin RI, Lux SE, Stossel TP, eds. Blood: Principles and Practice of Hematology. Philadelphia, PA: Lippincott; 1995:1701-1818.
12. Sung LA, Vera C. Protofilament and hexagon: a three-dimensional mechanical model for the junctional complex in the erythrocyte membrane skeleton. Ann Biomed Eng. 2003;31:1314-1326.
13. Fowler VM. Regulation of actin filament length in erythrocytes and striated muscle. Curr Opin Cell Biol. 1996;8:86-96.
14. Boukharov AA, Cohen CM. Guanine nucleotide-dependent translocation of RhoA from cytosol to high affinity membrane binding sites in human erythrocytes. Biochem J. 1998;330(pt 3):1391-1398.
15. Murphy MM, Zayed MA, Evans A, et al. Role of Rap1 in promoting sickle red blood cell adhesion to laminin via BCAM/LU. Blood. 2005;105:3322-3329.
16. Arthur WT, Quilliam LA, Cooper JA. Rap1 promotes cell spreading by localizing Rac guanine nucleotide exchange factors. J Cell Biol. 2004;167:111-122.
17. Pei X, An X, Guo X, Tarnawski M, Coppel R, Mohandas N. Structural and functional studies of interaction between *Plasmodium falciparum* knob-associated histidine-rich protein (KAHRP) and erythrocyte spectrin. J Biol Chem. 2005;280:31166-31171.
18. An X, Debnath G, Guo X, et al. Identification and functional characterization of protein 4.1R and actin-binding sites in erythrocyte beta spectrin: regulation of the interactions by phosphatidylinositol-4,5-bisphosphate. Biochemistry. 2005;44:10681-10688.
19. Fowler VM. Tropomodulin: a cytoskeletal protein that binds to the end of erythrocyte tropomyosin and inhibits tropomyosin binding to actin. J Cell Biol. 1990;111:471-481.
20. Gu H, Marth JD, Orban PC, Mossmann H, Rajewsky K. Deletion of a DNA polymerase beta gene segment in T cells using cell type-specific gene targeting. Science. 1994;265:103-106.
21. Steck TL. The organization of proteins in the human red blood cell membrane. A review. J Cell Biol. 1974;62:1-19.
22. Laemmli UK. Cleavage of structural proteins during the assembly of the head of bacteriophage T4. Nature (Lond). 1970;227:680-685.
23. Benard V, Bohl BP, Bokoch GM. Characterization of rac and cdc42 activation in chemoattractant-stimulated human neutrophils using a novel assay for active GTPases. J Biol Chem. 1999;274:13198-13204.
24. Gu Y, Jasti AC, Jansen M, Siefring JE. RhoH, a hematopoietic-specific Rho GTPase, regulates proliferation, survival, migration, and engraftment of hematopoietic progenitor cells. Blood. 2005;105:1467-1475.
25. Kuhlman PA, Fowler VM. Purification and characterization of an alpha 1 beta 2 isoform of CapZ from human erythrocytes: cytosolic location and inability to bind to Mg^{2+} ghosts suggest that erythrocyte actin filaments are capped by adducin. Biochemistry. 1997;36:13461-13472.
26. Ursitti JA, Fowler VM. Immunolocalization of tropomodulin, tropomyosin and actin in spread human erythrocyte skeletons. J Cell Sci. 1994;107(pt 6):1633-1639.
27. Clark MR, Mohandas N, Shohet SB. Osmotic gradient ektacytometry: comprehensive characterization of red cell volume and surface maintenance. Blood. 1983;61:899-910.
28. Mohandas N, Clark MR, Jacobs MS, Shohet SB. Analysis of factors regulating erythrocyte deformability. J Clin Invest. 1980;66:563-573.
29. Joiner CH, Jiang M, Claussen WJ, Roszell NJ, Yasin Z, Franco RS. Dipyridamole inhibits sickling-induced cation fluxes in sickle red blood cells. Blood. 2001;97:3976-3983.
30. Tuvia S, Levin S, Bitler A, Korenstein R. Mechanical fluctuations of the membrane-skeleton are dependent on F-actin ATPase in human erythrocytes. J Cell Biol. 1998;141:1551-1561.
31. Campanella ME, Chu H, Low PS. Assembly and regulation of a glycolytic enzyme complex on the human erythrocyte membrane. Proc Natl Acad Sci U S A. 2005;102:2402-2407.
32. Sugihara K, Nakatsuji N, Nakamura K, et al. Rac1 is required for the formation of three germ layers during gastrulation. Oncogene. 1998;17:3427-3433.
33. Glogauer M, Marchal CC, Zhu F, et al. Rac1 deletion in mouse neutrophils has selective effects on neutrophil functions. J Immunol. 2003;170:5652-5657.

34. Yang FC, Atkinson SJ, Gu Y, et al. Rac and Cdc42 GTPases control hematopoietic stem cell shape, adhesion, migration, and mobilization. Proc Natl Acad Sci U S A. 2001;98:5614-5618.
35. Sun CX, Downey GP, Zhu F, Koh AL, Thang H, Glogauer M. Rac1 is the small GTPase responsible for regulating the neutrophil chemotaxis compass. Blood. 2004;104:3758-3765.
36. Liu SC, Derick LH, Palek J. Visualization of the hexagonal lattice in the erythrocyte membrane skeleton. J Cell Biol. 1987;104:527-536.
37. Van Aelst L, D'Souza-Schorey C. Rho GTPases and signaling networks. Genes Dev. 1997;11: 2295-2322.
38. Jansen M, Yang FC, Cancelas JA, Bailey JR, Williams DA. Rac2-deficient hematopoietic stem cells show defective interaction with the hematopoietic microenvironment and long-term engraftment failure. Stem Cells. 2005;23:335-346.
39. Cancelas JA, Jansen M, Williams DA. The role of chemokine activation of Rac GTPases in hematopoietic stem cell marrow homing, retention and peripheral mobilization. Exp Hematol. 2006;34: 976-985.
40. Cho YJ, Zhang B, Kaartinen V, et al. Generation of rac3 null mutant mice: role of Rac3 in Bcr/Abl-caused lymphoblastic leukemia. Mol Cell Biol. 2005;25:5777-5785.
41. Corbetta S, Gualdoni S, Albertinazzi C, et al. Generation and characterization of Rac3 knockout mice. Mol Cell Biol. 2005;25:5763-5776.
42. Kannan R, Yuan J, Low PS. Isolation and partial characterization of antibody- and globin-enriched complexes from membranes of dense human erythrocytes. Biochem J. 1991;278(pt 1):57-62.
43. Lutz HU, Bussolino F, Flepp R, et al. Naturally occurring anti-band-3 antibodies and complement together mediate phagocytosis of oxidatively stressed human erythrocytes. Proc Natl Acad Sci U S A. 1987;84:7368-7372.
44. Kuhlman PA, Hughes CA, Bennett V, Fowler VM. A new function for adducin. Calcium/calmodulin-regulated capping of the barbed ends of actin filaments. J Biol Chem. 1996;271:7986-7991.
45. Li X, Matsuoka Y, Bennett V. Adducin preferentially recruits spectrin to the fast growing ends of actin filaments in a complex requiring the MARCKS-related domain and a newly defined oligomerization domain. J Biol Chem. 1998;273: 19329-19338.
46. Weber A, Pennise CR, Babcock GG, Fowler VM. Tropomodulin caps the pointed ends of actin filaments. J Cell Biol. 1994;127:1627-1635.
47. Gardner K, Bennett V. A new erythrocyte membrane-associated protein with calmodulin binding activity. Identification and purification. J Biol Chem. 1986;261:1339-1348.
48. Dong L, Chapline C, Mousseau B, et al. 35H, a sequence isolated as a protein kinase C binding protein, is a novel member of the adducin family. J Biol Chem. 1995;270:25534-25540.
49. Bennett V, Gardner K, Steiner JP. Brain adducin: a protein kinase C substrate that may mediate site-directed assembly at the spectrin-actin junction. J Biol Chem. 1988;263:5860-5869.
50. Fukata Y, Oshiro N, Kinoshita N, et al. Phosphorylation of adducin by Rho-kinase plays a crucial role in cell motility. J Cell Biol. 1999;145:347-361.
51. Kimura K, Fukata Y, Matsuoka Y, et al. Regulation of the association of adducin with actin filaments by Rho-associated kinase (Rho-kinase) and myosin phosphatase. J Biol Chem. 1998;273:5542-5548.
52. Barkalow KL, Italiano JE Jr, Chou DE, Matsuoka Y, Bennett V, Hartwig JH. Alpha-adducin dissociates from F-actin and spectrin during platelet activation. J Cell Biol. 2003;161:557-570.
53. Matsuoka Y, Hughes CA, Bennett V. Adducin regulation. Definition of the calmodulin-binding domain and sites of phosphorylation by protein kinases A and C. J Biol Chem. 1996;271:25157-25166.
54. Matsuoka Y, Li X, Bennett V. Adducin is an in vivo substrate for protein kinase C: phosphorylation in the MARCKS-related domain inhibits activity in promoting spectrin-actin complexes and occurs in many cells, including dendritic spines of neurons. J Cell Biol. 1998;142:485-497.
55. Gardner K, Bennett V. Modulation of spectrin-actin assembly by erythrocyte adducin. Nature. 1987;328:359-362.
56. Gilligan DM, Sarid R, Weese J. Adducin in platelets: activation-induced phosphorylation by PKC and proteolysis by calpain. Blood. 2002;99:2418-2426.
57. van de Water B, Tijdens IB, Verbrugge A, et al. Cleavage of the actin-capping protein alpha-adducin at Asp-Asp-Ser-Asp633-Ala by caspase-3 is preceded by its phosphorylation on serine 726 in cisplatin-induced apoptosis of renal epithelial cells. J Biol Chem. 2000;275:25805-25813.